JACS
JOURNAL OF THE AMERICAN CHEMICAL SOCIETY

Subscriber access provided by ISTANBUL TEKNIK UNIV

Article

Jammed Acid#Base Reactions at Interfaces

Julianne M. Gibbs-Davis, Jennifer J. Kruk, Christopher T. Konek, Karl A. Scheidt, and Franz M. Geiger

J. Am. Chem. Soc., **2008**, 130 (46), 15444-15447 • DOI: 10.1021/ja804302s • Publication Date (Web): 29 October 2008

Downloaded from http://pubs.acs.org on February 8, 2009

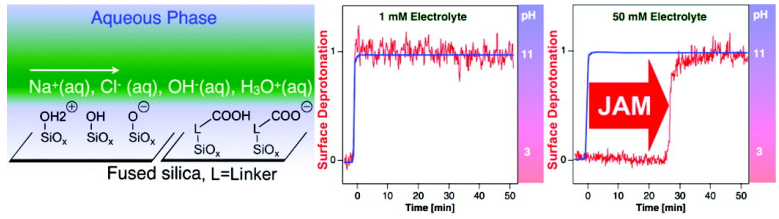

More About This Article

Additional resources and features associated with this article are available within the HTML version:

- Supporting Information
- Links to the 1 articles that cite this article, as of the time of this article download
- Access to high resolution figures
- Links to articles and content related to this article
- Copyright permission to reproduce figures and/or text from this article

View the Full Text HTML

ACS Publications
High quality. High impact.

Journal of the American Chemical Society is published by the American Chemical Society. 1155 Sixteenth Street N.W., Washington, DC 20036

J|A|C|S
ARTICLES

Published on Web 10/29/2008

Jammed Acid−Base Reactions at Interfaces

Julianne M. Gibbs-Davis, Jennifer J. Kruk, Christopher T. Konek, Karl A. Scheidt, and Franz M. Geiger*

Department of Chemistry, Northwestern University, 2145 Sheridan Road, Evanston, Illinois 60208

Received June 6, 2008; E-mail: geigerf@chem.northwestern.edu

Abstract: Using nonlinear optics, we show that acid−base chemistry at aqueous/solid interfaces tracks bulk pH changes at low salt concentrations. In the presence of 10 to 100 mM salt concentrations, however, the interfacial acid−base chemistry remains jammed for hours, until it finally occurs within minutes at a rate that follows the kinetic salt effect. For various alkali halide salts, the delay times increase with increasing anion polarizability and extent of cation hydration and lead to massive hysteresis in interfacial acid−base titrations. The resulting implications for pH cycling in these systems are that interfacial systems can spatially and temporally lag bulk acid−base chemistry when the Debye length approaches 1 nm.

Introduction

Interfacial acid−base processes are ubiquitous in nature.[1−6] Physical chemistry tells us that acid−base properties at interfaces should track acid−base properties in the bulk under equilibrium conditions. However, charge-balancing at the interface[7−9] as well as the molecular environments of the bulk and the interfacial species can shift interfacial acid−base equilibria by multiple pK_a units from their corresponding bulk solution values.[7,10−16] While a molecular-level understanding of these dramatic effects has now emerged for equilibrium, or steady-state conditions, their influence on the time dependence of interfacial acid−base reactions is just beginning to be understood. For instance, dynamic measurements using a surface force balance show that, following progressively longer waiting times after separation from contact, mica loses protons to approach its equilibrium charge state in water via an activated process that can be affected by the salt concentration in the surrounding aqueous solution.[17] While pH-sensitive chromophores diluted into surfactants at air/water interfaces have been studied as a function of electrolyte concentration,[7] time delays or hysteresis was not reported for those highly mobile two-dimensional systems. Hysteresis, however, was observed in electroosmotic measurements of silica capillaries[18] and calorimetric bulk equilibrium measurements on colloidal silica,[19] the latter of which can be rationalized using statistical rate theory.[20]

Here, we apply nonlinear optics to show that interfacial acid−base chemistry tracks the bulk pH at low salt concentrations. In the presence of 10 to 100 mM salt concentrations, however, the interfacial acid−base chemistry remains jammed for hours, until it finally occurs within minutes at a rate that follows the kinetic salt effect. For various alkali halide salts, the delay times increase with increasing anion polarizability and extent of cation hydration and lead to massive hysteresis in interfacial acid−base titrations.

Experimental Section

We use a flow system (Figure 1A) described previously[21,22] to monitor the interfacial protonation state in real time and in situ using an optical probe that is based on the "$\chi^{(3)}$ method".[12] The square root of the measured second harmonic generation (SHG)[23,24] intensity yields the SHG *E*-field, which depends on the interfacial potential, produced by the interfacial charges, whose density is given by the number density of the interfacial SiOH, SiO^-, and $SiOH_2^+$ groups (Figure 1B). For charged interfaces, the second harmonic generation (SHG) *E*-field can be modeled with the familiar second-order response to which a third-order term is added, according to $E_{SHG} = \chi^{(2)}E_\omega E_\omega - \chi^{(3)}E_\omega E_\omega \Phi_o$.[12] The third-order response is given by the product of the third-order nonlinear susceptibility, $\chi^{(3)}$, the

(1) Hynes, J. T. *Nature* **1999**, *397*, 565.
(2) Eigen, M. *Angew. Chem., Int. Ed. Engl.* **1964**, *3*, 1.
(3) Pearson, R. G. *J. Am. Chem. Soc.* **1963**, *85*, 3533.
(4) Bordwell, F. G. *Acc. Chem. Res.* **1988**, *21*, 456.
(5) Stumm, W.; Morgan, J. J. *Aquatic Chemistry, Chemical Equilibria and Rates in Natural Waters*, 3rd ed.; John Wiley & Sons: New York, 1996.
(6) Raviv, U.; Laurat, P.; Klein, J. *Nature* **2001**, *413*, 51.
(7) Xiao, X. D.; Vogel, V.; Shen, Y. R. *Chem. Phys. Lett.* **1989**, *163*, 555.
(8) Uibel, R. H.; Harris, J. M. *Anal. Chem.* **2002**, *74*, 5112.
(9) Huang, X.; Kovaleski, J. M.; Wirth, M. J. *Anal. Chem.* **1996**, *68*, 4119.
(10) Bhattacharyya, K.; Sitzmann, E. V.; Eisenthal, K. B. *J. Chem. Phys.* **1987**, *87*, 1442.
(11) Bain, C. D.; Whitesides, G. M. *Langmuir* **1989**, *5*, 1370.
(12) Zhao, X.; Subrahmanyan, S.; Eisenthal, K. B. *Chem. Phys. Lett.* **1990**, *171*, 558.
(13) Zhao, X.; Ong, S.; Wang, H.; Eisenthal, K. B. *Chem. Phys. Lett.* **1993**, *214*, 203.
(14) Hu, K.; Bard, A. J. *Langmuir* **1997**, *13*, 5114.
(15) Gershevitz, O.; Sukenik, C. N. *J. Am. Chem. Soc.* **2004**, *126*, 482.
(16) Konek, C. T.; Musorrafiti, M. J.; Al-Abadleh, H. A.; Bertin, P. A.; Nguyen, S. T.; Geiger, F. M. *J. Am. Chem. Soc.* **2004**, *126*, 11754.
(17) Raviv, U.; Laurat, P.; Klein, J. *J. Chem. Phys.* **2002**, *116*, 5167.
(18) Lambert, W. J.; Middleton, D. L. *Anal. Chem.* **1990**, *62*, 1585.
(19) Machesky, M. L.; Anderson, M. A. *Langmuir* **1986**, *2*, 582.
(20) Piasecki, W. *Langmuir* **2003**, *19*, 9526.
(21) Mifflin, A. L.; Gerth, K. A.; Geiger, F. M. *J. Phys. Chem. A* **2003**, *107*, 9620.
(22) Al-Abadleh, H. A.; Mifflin, A. L.; Musorrafiti, M. J.; Geiger, F. M. *J. Phys. Chem. B* **2005**, *109*, 16852.
(23) Shen, Y. R. *The Principles of Nonlinear Optics*; John Wiley & Sons: New York, 1984.
(24) Eisenthal, K. B. *Chem. Rev.* **1996**, *96*, 1343.

10.1021/ja804302s CCC: $40.75 **© 2008 American Chemical Society**

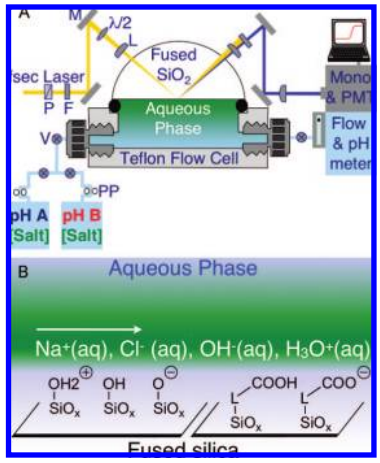

Figure 1. Experimental setup and illustration of the interface. (A) Experimental setup: The laser system consists of an optical parametric amplifier driven by a kilohertz regeneratively amplified diode-pumped Ti: sapphire laser system (Spectra Physics/Newport) producing 120 fs pulses that are directed onto a fused silica/water interface at pulse energies below 2 μJ, which is well below the damage threshold when using a 50 μm spot size. P = polarizer, F = filter, 1/2 = half-wave plate, L = lens, M = mirror, PP = peristaltic pump, Mono = monochromator, PMT = photomultiplier. All experiments are carried out at room temperature and in duplicate on five different fused silica hemispheres. (B) Charged and neutral species at silica/water interfaces and those functionalized with organic acids (L = linker) in the presence of a flowing bulk aqueous phase containing electrolyte (sodium chloride) adjusted to a given bulk pH. The presence of the diffuse electrical double layer is indicated by the color gradient.

two applied electromagnetic probe fields oscillating at frequency ω, E_ω, and the interfacial potential, Φ_o, which is produced by the interfacial charges, the corresponding spatial distribution of the counter charges, and dipolar arrays of aligned water molecules. The localization of the protonatable and deprotonatable groups at the interface and the high sensitivity of the $\chi^{(3)}$ method to the interfacial potential make the experiment interface specific.

The signal detection formalism corresponds to a heterodyne detection scheme. At a given bulk solution pH, the interface contains a corresponding number of charged and neutral species (Figure 1B) consisting of either SiOH, SiO^-, and $SiOH_2^+$ groups[25] in the case of the fused silica/water interfaces, or of Si−R−COOH and Si−R−COO^- groups[4] in the case of the amino-acid-functionalized fused silica/water interfaces. By modulating the pH of the bulk solution, the relative populations of these different surface sites change, which leads to a change in the overall charge density and consequently the interfacial potential. On a molecular level, the interfacial potential aligns the water molecules within the diffuse electrical double layer that is presumably set up at a charged aqueous/solid interface.[26] The $\chi^{(3)}$ response of the interfacial water molecules, whose structure[27,28] and dynamics[29] have been determined using sum frequency generation, can then contribute to the SHG *E*-field produced at the interface. If the experiments are carried out at constant pH and varying salt concentration, the measured SHG *E*-field response yields the interfacial charge density via various electrical double-layer models.[7,12,16,30]

Results and Discussion

Figure 2A,B shows that bulk pH jumps between 3 and 11 change the SHG *E*-field. We reference the time-dependent SHG *E*-field to the SHG *E*-field recorded before the jump, which occurs at $t = 0$ min, and normalize to the SHG *E*-field at $t =$ 50 min after the jump. If the bulk salt concentration is maintained at 1 mM, the interfacial protonation state tracks the bulk pH; that is, the pH in the bulk and at the interface change simultaneously (Figure 2A). However, when the bulk salt concentration is increased to 50 mM, the interfacial response is substantially delayed with respect to the bulk pH jump (Figure 2B). The salt concentration dependence of the time delays observed here is reminiscent of that reported for block-copolymer dissociation triggered by pH 12 to 4 jumps, which shows second-long time delays when salt is present at 1.0 M but none in its absence.[31] Control studies (see Supporting Information) indicate that mixing conditions, dissolution, impurities, or laser heating or instabilities are unlikely causes for the delay times. Furthermore, initiating small pH jumps or anion or cation adsorption experiments near neutral conditions do not result in time delays, even at 0.5 M salt concentrations. Instead, we find that the delay times are overwhelmingly controlled by the difference in the initial and final pH values, the salt concentration, and the chemical composition of the alkali halide salt used in the experiments.

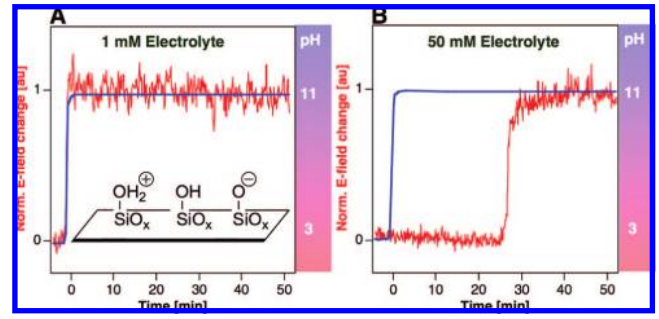

Figure 2. Normalized SHG *E*-field change referenced to the SHG *E*-field at $t = 0$ min (left axis, thin trace) recorded as a function of time from fused silica/water interfaces at electrolyte concentrations of 1 mM (A) and 50 mM (B) for pH jumps (right axis, thick trace) between 3 and 11. To maintain constant ionic strength, HCl and NaOH stock solutions of the same NaCl bulk concentration are used to adjust the pH; $\lambda_{SHG} = 300$ nm. The polarization combination was p-in/all-out, and the bulk flow rate was held at 0.3 mL/s.

We analyze the SHG versus time traces recorded during the pH jumps by sigmoidal fits of the form $y = 1/[1 + n \times \exp(r(\tau - t)]$. Here, y is the SHG *E*-field change, n is a fit parameter related to the initial and final SHG *E*-field change, and r is the rate of the SHG *E*-field change. The inflection point of the s-shaped time traces is located at the delay time τ. Figure 3A shows that the delay times increase until the salt concentration reaches about 100 mM, after which they last, on average, 100 min with a standard deviation of 20 min (Figure 3B).

Consistent with the notion that the interfacial negative charge density[13,25] is higher at pH 11 than at pH 3, which is close to the point of zero charge (pzc, ~2 for fused silica),[32] the delay times are two to three times shorter for the pH 11 to 3 jumps than for the reverse jumps. Similarly, the rates of the SHG *E*-field change are about two times faster for the pH 11 to 3

(25) Duval, Y.; Mielczarski, J. A.; Pokrovsky, O. S.; Mielczarski, E.; Erhrhardt, J. J. *J. Phys. Chem. B* **2002**, *106*, 2937.
(26) Adamson, A. W. *Physical Chemistry of Surfaces*, 5th ed.; John Wiley & Sons: New York, 1990.
(27) Gopalakrishnan, S.; Liu, D.; Allen, H. C.; Kuo, M.; Shultz, M. J. *Chem. Rev.* **2006**, *106*, 1155.
(28) Scatena, L. F.; Brown, M. G.; Richmond, G. L. *Science* **2001**, *292*, 908.
(29) McGuire, J. A.; Shen, Y. R. *Science* **2006**, *313*, 1945.
(30) Boman, F. C.; Musorrafiti, M. J.; Gibbs, J. M.; Stepp, B. R.; Salazar, A. M.; Nguyen, S. T.; Geiger, F. M. *J. Am. Chem. Soc.* **2005**, *127*, 15368.
(31) Zhu, Z.; Xu, J.; Zhou, Y.; Jiang, X.; Armes, S. P.; Liu, S. *Macromolecules* **2007**, *40*, 6396.
(32) Parks, G. A. *Chem. Rev.* **1965**, *65*, 177.

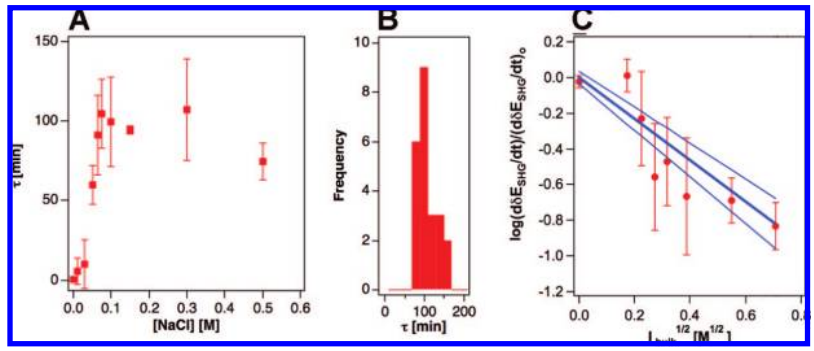

Figure 3. (A) Delay times for the SHG *E*-field versus time traces as a function of increasing electrolyte concentration for pH jumps starting at 3 and ending at 11. (B) Histogram of time delays recorded for salt concentrations above 100 mM. (C) Logarithm of the rate of the SHG *E*-field change as a function of the square root of the ionic strength for pH 3 to 11 jumps. The thick straight line is the best fit to a linear function of the form $y = ax + b$, and the thin straight lines are the upper and the lower bounds resulting from the fit.

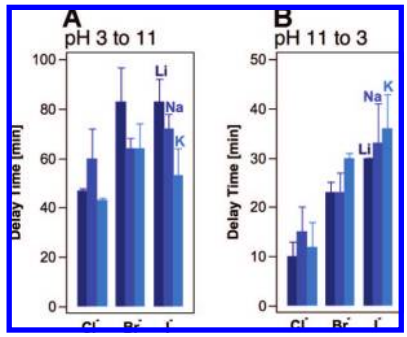

Figure 4. Delay times for (A) pH 3 to 11 jumps and (B) pH 11 to 3 jumps measured for various 50 mM alkali metal halide solutions.

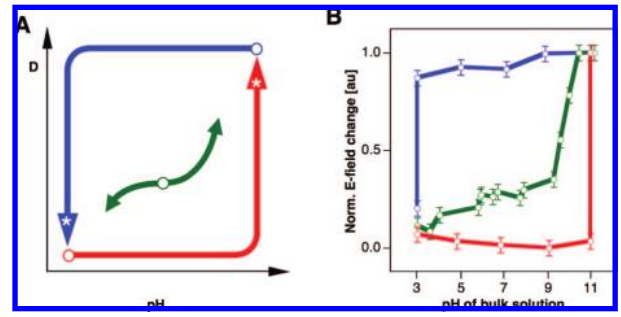

Figure 5. Hysteresis at the silica/water interface. (A) Predicted steady-state (green curved arrows) and non-steady-state (blue and red bent arrows) acid−base surface titration experiment. D is the degree of deprotonation; the empty circles and the white stars indicate initial and final pH conditions, respectively, and the direction of the pH change is indicated by the direction of the arrows and the blue and red colors. (B) SHG *E*-field change referenced to the lowest SHG *E*-field and normalized to the maximum SHG *E*-field recorded during the acid−base surface titration of the fused silica/water interface. The experiments are carried out at a flow rate of 0.3 mL/s and an electrolyte concentration of 0.5 M. They are initiated at neutral pH (green filled circles) and at pH 3 (red empty squares) or 11 (blue filled squares). When starting at pH 3 or 11, the steady-state response is reached after up to 4.5 h and once the final pH (11 or 3) is reached.

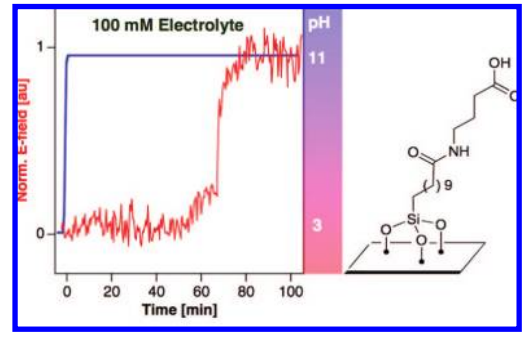

Figure 6. Normalized SHG *E*-field change (left axis, thin trace) versus time trace from fused silica/water interfaces functionalized with γ-amino butyric acid (GABA) subjected to bulk solution pH jumps (right axis, thick trace) between pH 3 and 11 at an electrolyte concentration of 0.1 M NaCl.

jumps than for the reverse jumps. Reflecting the importance of charge−charge interactions between the aqueous and the interfacial reactants, the rates depend on the bulk ionic strength and follow the kinetic salt effect[33] (Figure 3C). The negative slopes, which indicate oppositely charged reactants, yield absolute reactant charge valences ranging from 0.99 to 1.29, consistent with the presence of OH^- and $SiOH^{2+}$.

Using various 50 mM alkali halide salts, we find that the rate of the SHG *E*-field change does not depend on which alkali halide salt is used in the experiment. The delay times, however, show a clear dependence on the choice of the alkali cation and the halide anion. The pH 3 to 11 jumps begin with an interface that is only slightly negatively charged, and cations and anions should be present at comparable number densities near the interface. Small cations such as lithium, which are strongly hydrated,[34] are expected to rigidify the interfacial water structure within the diffuse electrical double layer, while larger cations such as potassium should form less rigid interfacial water structures. If the delay times were to correlate with the rigidity of the interfacial water structure, then strongly hydrated cations should result in longer delay times than weakly hydrated cations. The data shown in Figure 4A are consistent with this scenario, especially when bromide or iodide is used as the anion, the latter leading to delay time increases by up to 30 min when switching from lithium to potassium.

In pH 11 to 3 jumps, the experiment begins with a high interfacial density of negative charge to which the alkali cations should be attracted while the halide anions are located further away toward the aqueous phase. Similar to what is observed in equilibrium experiments addressing halide adsorption to water/vapor interfaces,[35] an important property to consider for the anions may be their polarizability. With respect to the incoming

(33) Atkins, P. W. *Physical Chemistry*, 6th ed.; Oxford University Press: New York,1998.
(34) Hofmeister, F. *Arch. Exp. Pathol. Pharmakol. (Leipzig)* **1888**, *24*, 247.
(35) Ghosal, S.; Hemminger, J. C.; Bluhm, H.; Mun, B. S.; Hebenstreit, E. L. D.; Ketteler, G.; Ogletree, D. F.; Requejo, F. G.; Salmeron, M. *Science* **2005**, *307*, 563.

hydronium ions, the rigidity of the interfacial water structure would then be primarily given by the magnitude of the induced dipole moments set up within the adsorbed anions. The data shown in Figure 4B are consistent with this scenario: the delay times increase by up to 250% when going from less polarizable chloride to more polarizable iodide, while the dependence of the delay times on the extent of cation hydration is much less pronounced. We note that a rigid interfacial water structure and screening of the charged surface sites should decrease the driving force for the acid−base reactions. Conversely, faster bulk supply rates of the hydronium or hydroxide ions should decrease the delay times and increase the rate at which the aqueous ions penetrate the interfacial water structure. This is indeed observed for 50 mM salt concentrations but not for 0.5 M salt concentrations (see Supporting Information), where the delay times and rates are largely insensitive to the bulk flow rate. As expected, stirring to turbulent flow conditions is found to disrupt the structure of the charged double layer and the interfacial acid/base chemistry responds instantaneously, independently of the salt concentration used.

The results presented here suggest that surface acid−base titrations should depend on the starting bulk pH condition and the extent of the pH jump (Figure 5A). We illustrate this path dependence by first initiating pH jumps covering less than two pH units near neutral conditions. Clear time delays are not observed even at 0.5 M salt concentrations, and the steady-state interfacial acid−base titration curve first reported by Eisenthal and co-workers[13] is obtained.

When we now begin the interfacial acid−base titration experiment under acidic (pH 3) or basic (pH 11) conditions instead of neutral pH, we observe massive hysteresis. In these experiments, we carry out four pH jumps, each covering two pH units. After each pH jump, we wait for up to 1 h while recording the SHG *E*-field versus time trace. Figure 5B clearly shows that the SHG *E*-field does not change until the bulk pH reaches either 11 or 3, at which point up to 4.5 h have passed. When the SHG *E*-field finally changes, it reaches the steady-state level that is obtained for pH 11 or 3 when initiating acid−base titrations at neutral pH. We note here that pH jumps initiated at pH 3 or 11 spanning less than eight pH units should eventually result in interfacial protonation state changes, but this process takes up to 1 h at 50 mM salt and at 0.5 M salt was not observed during the duration of the 5-h experiment. These observations suggest that the differences in bulk solution pH must be substantial if the interface is to respond within reasonable time scales at high salt concentrations.

We note that the $(1\bar{1}02)$ α-alumina/water interface, which possesses a higher pzc value (5.2) than fused silica,[32,36] shows the same qualitative albeit shorter time delay (see Supporting Information), indicating, as expected, that the pzc value plays an important role. Finally, the time delays also exist for organic acid−base systems. In this case, we functionalize a fused silica/water interface with γ-amino butyric acid (GABA).[37] The pH jumps between 3 and 11 carried out at high electrolyte concentration lead to time delays (Figure 6) and hysteresis (Supporting Information) that are similar to what we observe for the inorganic systems at comparable salt concentrations. These observations suggest that the dynamic response behavior may be general for many acid−base equilibrium involving surface-localized and immobile species under electrolyte solution.

Conclusions

The dynamic and steady-state experiments presented here show that salt can jam interfacial acid−base chemistry for hours. As a result, the interfacial protonation states of surface-bound acids and bases are shifted much further away from their corresponding bulk values than what had been known previously about these systems under steady-state conditions.[11−15] The effect requires flow rates and electrolyte concentrations that are prevalent in atmospheric aerosol chemistry, heterogeneous contaminant processing in geochemistry, drug design and delivery in medicine, and biodetection and sensor function in biodiagnostics. The resulting implications for pH cycling in these systems are that interfacial systems can spatially and temporally lag bulk acid−base chemistry when the Debye length approaches 1 nm.

Acknowledgment. This work was supported by the Director, Chemical Sciences, Geosciences and Biosciences Division, of the U.S. Department of Energy under Grant No. DE-FG02-06ER15787, the National Science Foundation under Experimental Physical Chemistry CAREER Grant No. CHE-0348873, the Camille & Henry Dreyfus Foundation Environmental Chemistry Postdoctoral Program (J.G.D.), the Northwestern University Nanoscale Science and Engineering Center, and the Sloan Foundation (K.A.S. and F.M.G.).

Supporting Information Available: Details regarding the cell geometry, cleaning procedures, impurity assessments and control studies, and SHG *E*-field referencing and normalization proceduces. This material is available free of charge via the Internet at http://pubs.acs.org.

JA804302S

(36) Musorrafiti, M. J.; Konek, C. T.; Hayes, P. L.; Geiger, F. M. *J. Phys. Chem. C* **2008**, *112*, 2032.
(37) Gibbs-Davis, J. M.; Hayes, P. L.; Scheidt, K.; Geiger, F. M. *J. Am. Chem. Soc.* **2007**, *129*, 7175.